

## Photoreactivity of Si(111)–H in Ambient

D. Bodlaki and E. Borguet\*

*Department of Chemistry, Temple University, Philadelphia, Pennsylvania 19122*

*Received: June 23, 2006; In Final Form: September 19, 2006*

Second harmonic generation rotational anisotropy (SHG-RA) provides a convenient means to monitor the chemical state of the Si surfaces and to follow the conversion of a H-terminated surface to  $\text{SiO}_2$  by oxidation as a function of time in ambient. SHG at 800 nm is sensitive to changes in the surface electronic properties induced by oxidation, and it probes both the initial stage of oxidation and the logarithmic oxide growth. We found that intense, ultrashort (4 ps) 800 nm laser pulses accelerate the initial stage of oxidation of Si(111)–H in ambient. The cross-section of the photoinduced process was found to be  $(1.7 \pm 0.5) \times 10^{-23} \text{ cm}^2$ . A mechanism involving drift of photoexcited electrons toward the surface is proposed to explain the photooxidation.

### Introduction

The passivation of semiconductor interfaces and the stability of passivated interfaces under reactive conditions are topics of research for physical scientists and technologists alike.<sup>1,2</sup> Remarkably, it has been shown that atomically flat passivated Si(111) surfaces can be generated by simple wet chemical techniques.<sup>3</sup>  $\text{NH}_4\text{F}$  solutions can terminate the Si dangling bonds by H atoms to form monohydride Si species on Si(111).<sup>3</sup> This passivated surface is the starting point for a number of processes that transform the chemical and physical nature of the semiconductor interface.<sup>4</sup> Thus, stability of H-terminated surfaces is of interest.

At the same time, attachment of organic molecules to Si surfaces has attracted attention.<sup>4–9</sup> The wet chemical grafting of organic molecules to silicon interfaces invariably starts with a H-passivated Si surface.<sup>4,8,9</sup> Thus, the controlled removal or replacement of H on the Si surface is a widely sought after goal.<sup>4,8</sup> The removal of hydrogen from Si surfaces has been achieved by a number of different means including STM<sup>10</sup> and laser irradiation.<sup>11–13</sup> There has been considerable theoretical effort to understand these processes.<sup>14,15</sup> Thermal and nonthermal, photon driven removal of H has been shown to result in quite different surfaces.<sup>16</sup> Direct single photon desorption of H from Si surfaces in UHV has been reported with 157 nm (7.9 eV) photons.<sup>13</sup> Desorption of H from Si surfaces by 308 nm (4.0 eV) photons was proposed to proceed via a thermal process, although the nonlinear fluence dependence was also consistent with a multiphoton mechanism.<sup>11</sup> However, Chidsey et al. suggested, in light of their results with low intensity near UV photons (>3.5 eV), that a low cross-section single photon mechanism might also contribute to H desorption from Si(111).<sup>17</sup> Thus, the mechanism of photoassisted H desorption with photon energies <7.9 eV is still debated.

The photoreactivity of H–Si(111) has been exploited by Chidsey et al. to functionalize silicon surfaces.<sup>17</sup> Illumination of H–Si(111) with low intensity ( $\text{mW}/\text{cm}^2$ ) UV light ( $\lambda < 350 \text{ nm}$ ) in air results in oxidized Si. Longer wavelengths reportedly produced no oxidation.<sup>17</sup> The proposed mechanism was based on photocleavage of the Si–H bond, whose bond strength (79–84 kcal/mol, 3.42–3.59 eV, 362–345 nm) has approximately

the energy of a 350 nm photon.<sup>18</sup> A detailed radical chain mechanism was proposed involving the creation of a surface radical, a dangling Si bond formed by photocleavage of the Si–H bond.<sup>17</sup> Unsaturated compounds, e.g.,  $\text{O}_2$  and alkenes, can then react with the Si dangling bond.<sup>17</sup> The resultant adsorbate-based radical then abstracts a neighboring surface hydrogen with the creation of another Si dangling bond, thereby propagating the reaction.<sup>17</sup> However, the mechanism of Si–H bond photocleavage is not clear. Direct photodissociation of the Si–H bond requires ~7.9 eV photons, an energy much greater than the ~3.5 eV photons that result in photoreactivity of the Si(111) surface.<sup>12,13</sup>

Given the photoreactivity of H–Si(111), the perturbation induced by optical measurement techniques is of concern. In one recent study of the stability of H–Si(111) in air, by infrared + visible sum frequency generation, it was shown that the intensity of the Si–H stretch vibrational band decreased under irradiation by 532, 1064, and 4794 nm photons.<sup>19</sup> The shorter the photon wavelength employed, the greater the rate of decrease of the SiH vibrational feature was.<sup>19</sup> Under conditions of low power irradiation [8  $\mu\text{J}$  visible (532 nm; beam area, 0.018  $\text{cm}^2$ ; repetition rate, 10 Hz; and pulse duration, 25 ps) and 30  $\mu\text{J}$  IR (4794 nm; beam area, 0.0005  $\text{cm}^2$ ; repetition rate, 10 Hz; and pulse duration, 25 ps)], no effect of laser irradiation was detected on the SFG response in the first 60 min.<sup>19</sup> However, a further 90 min of laser irradiation resulted in a reduction of SFG peak height to 15% of the original value.<sup>19</sup> The observed induction time suggested a nucleation and growth mechanism.<sup>19</sup> The low initial abstraction rate ( $3.8 \times 10^{-5} \text{ ML/s}$  at 17  $\mu\text{J}$  vis-532 nm, 25  $\mu\text{J}$  IR-4794 nm) is consistent with the laser-induced desorption rate ( $< 10^{-6} \text{ ML/pulse}$ ) reported by Guyot-Sionnest in UHV.<sup>20</sup> The abstraction rate was observed to depend nonlinearly on laser energy.<sup>19</sup> It was also reported that moisture significantly affected the stability of H–Si(111) under laser illumination; degradation of H–Si(111) immersed in water was reported to be significantly accelerated.<sup>19</sup>

Somewhat surprisingly, the SFG signal was observed to decrease as a function of time when the IR intensity was increased.<sup>19</sup> Indeed, the effect of the IR photons appeared to be even greater than that of 1064 nm photons.<sup>19</sup> As the Si substrate does not absorb at 4090 nm, it was not clear whether the photoinduced process was indeed a substrate- or an adsorbate-

\* To whom correspondence should be addressed.

mediated process or perhaps even the result of the nonlinear response.<sup>21</sup> While the absorption coefficient of bulk Si is about 3 orders of magnitude less for 1064 nm photons as compared with 532 nm photons, the observed abstraction rate constant differs by only about an order of magnitude ( $0.27 \times 10^{-4} \text{ s}^{-1}$  at 1064 nm vs  $3.5 \times 10^{-4} \text{ s}^{-1}$  at 532 nm) when compared on the basis of equal pulse energies.<sup>19,21</sup>

In this paper, we demonstrate that photooxidation of H-Si(111) can be induced by 800 nm photons and can be investigated by second harmonic generation (SHG). We show that this is not a multiphoton process and that it requires the presence of oxygen. The influence of water vapor is also investigated.

## Experimental Section

n-type Si(111) crystals (P doped with  $\sim 30 \Omega \text{ cm}$  resistivity, Motorola Phoenix,  $\sim 300 \mu\text{m}$  thick) were used in the experiments. H termination involved the following steps: cleaning in piranha solution [4:1 concentrated  $\text{H}_2\text{SO}_4$  (Fisher, Trace Metal Grade):30%  $\text{H}_2\text{O}_2$  (J. T. Baker, CMOS grade)] for 10 min at  $100^\circ\text{C}$ , followed by an SC2 clean [1:1:4 30%  $\text{H}_2\text{O}_2$ :concentrated HCl (J. T. Baker, CMOS grade): $\text{H}_2\text{O}$ ] for 10 min at  $80^\circ\text{C}$ , and finally a further 10 min in piranha solution at  $100^\circ\text{C}$ . At the end of the sequence, the samples were thoroughly rinsed in deionized water ( $> 18 \text{ M}\Omega \text{ cm}$ ).<sup>22</sup> For H termination, the samples were immersed in 40%  $\text{NH}_4\text{F}$  solution (Transene, Semiconductor Grade) for 15 min to remove oxide and H terminate the surface Si.<sup>23</sup> After immersion in  $\text{NH}_4\text{F}$ , the samples were hydrophobic, as noted by the ease with which water rolled off of the samples. Native oxide samples, which were used as received, were only subjected to a degreasing in trichloroethylene, acetone, and methanol for 10 min each at room temperature prior to experiments.

The ellipsometric thickness was measured on a Gaertner Scientific ellipsometer (model L117) at a  $70^\circ$  angle of incidence and  $\lambda = 632.8 \text{ nm}$ . A typical ellipsometric thickness of native oxide Si(111) samples was  $2.0 \pm 0.05$  and  $0.5 \pm 0.3 \text{ nm}$  for H-terminated Si(111). We used  $n = 3.882$ ,  $k = 0.019$  for Si and  $n = 1.455$  for  $\text{SiO}_2$  at  $632.8 \text{ nm}$  when calculating layer thickness.<sup>21</sup> Advancing water contact angles were measured, within 10 s, with a VCA-2000 contact angle goniometer. The typical contact angle of Si(111)/ $\text{SiO}_2$  after degreasing was  $60 \pm 10^\circ$ . The hydrophobic character of Si(111)-H was confirmed by the high contact angle ( $99 \pm 6^\circ$ ).

Second harmonic generation rotational anisotropy (SHG-RA) measurements were carried out to control the quality of the crystal cut and the effect of wet chemical treatment.<sup>24,25</sup> In these measurements, the  $0^\circ$  azimuthal angle was set equal to the  $[2\bar{1}\bar{1}]$  direction. SHG-RA measurements were measured with 4 ps pulses from a Ti:sapphire regenerative amplifier operating at 1 kHz.<sup>26</sup> The p-polarized 800 nm beam was incident on the sample at  $45^\circ$  with respect to the surface normal. The experimental conditions were chosen such that the illuminated spot was at least 2 mm away from the axis of rotation. Thus, each data point in the SHG-RA experiment received less than 20 s of illumination in the SHG-RA measurement. The fluence was typically  $7 \text{ mJ/cm}^2$  unless otherwise noted, generating an initial excited carrier density of  $2 \times 10^{19} \text{ cm}^{-3}$  near the surface.<sup>27</sup> The beam was optically filtered (Kopp Glass Inc. #2-63) to remove second harmonic photons (400 nm) and lightly focused to a beam diameter, determined using a knife edge technique, of  $1.1 \pm 0.1 \text{ mm}$ . The beam area was corrected for the elliptical shape obtained at nonnormal incidence. The reflected beam was sent to a monochromator (Acton Research, 300i, 2400 gr/mm grating) after short pass filtering (Kopp Glass Inc. #4-94) to block 800 nm photons. A liquid nitrogen-cooled CCD camera

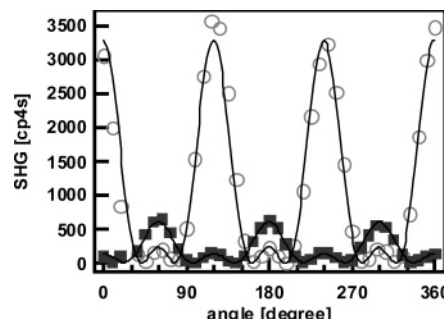


**Figure 1.** SHG rotational anisotropy pattern of H-terminated (■) and oxide-covered (○) Si(111) surfaces recorded in air ambient (RH = 40%). The  $0^\circ$  azimuth coincides with the  $[2\bar{1}\bar{1}]$  direction.

(Princeton Instrument, CCD30-11) was used in single element detection mode. An analyzing polarizer was set to pass p-polarized SH photons. The quadratic nature of the second harmonic response was verified in the power range explored.<sup>28</sup>

## Results and Discussion

The H-terminated and oxide-covered Si(111) surfaces can be distinguished via their distinct SHG-RA shown in Figure 1. In addition to displaying a quite distinct pattern, the overall magnitude of the SHG-RA of H-Si(111) is much smaller than that for oxide-covered Si(111) surfaces. The SHG-RA pattern can be interpreted by the following phenomenological formula

$$I_{pp}(2\omega) \propto |A_{pp} + B_{pp} \cos(3\phi)|^2 \quad (1)$$

where  $A_{pp}$  and  $B_{pp}$  are the isotropic and anisotropic contributions to the nonlinear susceptibility, respectively.<sup>29</sup>  $A_{pp}$  and  $B_{pp}$  parameters are complex numbers, whose relative phase  $\Delta_{AB}$  can be defined via

$$\frac{A_{pp}}{B_{pp}} = \frac{|A_{pp}|}{|B_{pp}|} \exp(i\Delta_{AB}) \quad (2)$$

The pattern is, in part, the result of an interference between the complex  $A_{pp}$  and  $B_{pp}$  terms. The reversal in the sequence of large peaks and small peaks in the SHG-RA patterns for H-Si(111) and  $\text{SiO}_2/\text{Si}(111)$  is primarily a consequence of the different relative phase between  $A_{pp}$  and  $B_{pp}$  for the two systems:  $12^\circ$  for Si(111)- $\text{SiO}_2$  and  $162^\circ$  for Si(111)-H.

By monitoring the SHG signal at an azimuth of  $0^\circ$ , one can follow the photooxidation of the surface. This azimuthal orientation provides the greatest contrast between the H-terminated and the oxide-covered Si(111) surfaces, as can be seen by inspection of Figure 1. Under ambient conditions (RH =  $40 \pm 5\%$ ), continuous illumination by 800 nm photons from the 4 ps laser results in a slight decrease of the SHG signal at the  $0^\circ$  azimuth in the first 50 min (Figure 2, inset). At the same time, a significant decrease of the SHG signal by a factor of 3 is observed at the  $60^\circ$  azimuth.<sup>24</sup> The behavior at the  $0^\circ$  and  $60^\circ$  azimuth is consistent with oxidation of the surface. Under our illumination conditions, a flux of  $8.4 \times 10^{19} \text{ photon s}^{-1} \text{ cm}^{-2}$  of 800 nm photons, there is no sign of the induction time reported by Ye et al. for fluxes of  $1.2 \times 10^{16} \text{ photon s}^{-1} \text{ cm}^{-2}$  of 532 nm photons and  $1.4 \times 10^{19} \text{ photon s}^{-1} \text{ cm}^{-2}$  of 4794 nm photons.<sup>17</sup> The initial slight decrease is followed by an increase of the SHG signal with time (Figure 2, curve a). The SHG signal begins to level off after 7 h. We attribute the changes in the SHG signal to photooxidation. This is supported by the SHG-RA pattern, recorded after illumination by 800 nm

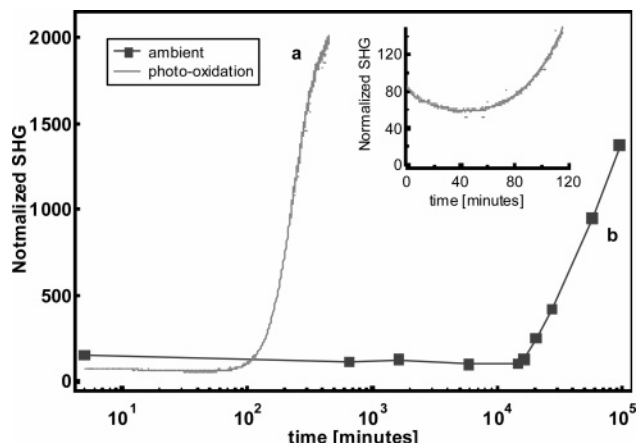


**Figure 2.** SHG response at 0° azimuth for H-terminated Si(111) surfaces in ambient under continuous illumination ( $20.6 \text{ mJ/cm}^2$ ) (—) and intermittent laser irradiation, i.e., sampled on average every 3 days after H termination (■). Each data point in the intermittent experiment received less than 20 s of illumination ( $7 \text{ mJ/cm}^2$ ). The SHG signal was recorded at the 0° azimuth of Figure 1.

photons, which shows a pattern similar to that of the oxide but with the SHG intensity reduced by a factor of 2 (Figure 2).<sup>24</sup>

The effect of ambient oxidation is slower, as verified in control experiments.<sup>24</sup> To investigate only the effect of the ambient on the oxidation, the SHG-RA of a Si(111)-H was taken as rarely as possible, on average every 3 days after H termination (Figure 2, curve b). Care was taken in choosing the SHG-RA experimental conditions such that the illuminated spot was at least 2 mm away from the axis of rotation. Thus, each data point in the SHG-RA experiment received less than 20 s of illumination, resulting in negligible photoreaction (insertion of <0.005 ML oxygen) as a consequence of each SHG-RA measurement.<sup>24</sup> The SHG intensity at the 0° azimuth plotted against the time the sample was exposed to air is shown in Figure 2 (curve b). The period of slow SHG signal variation, an initial decrease followed by an increase, was found to be ~200 times longer for ambient oxidation than for laser-induced oxidation when using  $268 \mu\text{J}/\text{pulse}$  energy ( $21 \text{ mJ/cm}^2$ ). More detailed studies of the ambient oxidation of H-Si(111) are reported elsewhere.<sup>24</sup>

The oxygen coverage was estimated via a correlation determined between the phase,  $\Delta_{AB}$ , and the oxide thickness determined by ellipsometry.<sup>24</sup> Both the phase  $\Delta_{AB}$  and the oxide thickness showed slow-fast-slow evolution with time, which has been described previously.<sup>30–35</sup> Graf et al. investigated the oxidation of H-Si(100) under varying reaction conditions, e.g., immersed in water and in air.<sup>30,31</sup> They found that the oxygen coverage corresponding to the transition region between the slow and the fast growth kinetics is about the same in water ( $6 \times 10^{14} \text{ O atom/cm}^2$ ) and in air ( $4 \times 10^{14} \text{ O atom/cm}^2$ ).<sup>30,31</sup> The density of interface atoms at the Si(100) surface is  $7 \times 10^{14} \text{ atom/cm}^2$ .<sup>35</sup> Therefore, it can be assumed that there is a critical coverage (~0.7 ML) after which the oxide growth is accelerated.<sup>31</sup> The rate of oxidation and photoreactive cross-section for oxidation can be determined by assuming that the onset of the fast increase of the SHG phase is actually characteristic of 0.7 ML oxide coverage surface. The rate of oxidation was calculated by dividing 0.7 ML by the duration of the slow phase of oxidation in seconds. The photoreactive cross-section at atmospheric pressure is given by the coverage 0.7 ML, divided by the number of photons absorbed to cause the photooxidation of 0.7 ML.

The number of absorbed photons is determined from the beam spot size, the photon irradiance, and the reflectivity of the

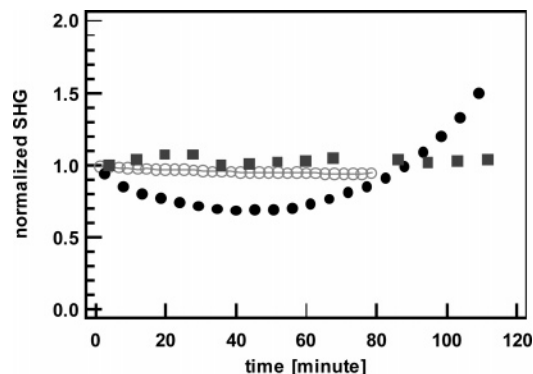


**Figure 3.** Time-dependent SHG signals for H-terminated (●) and oxide-covered (○) Si(111) surfaces in ambient, as well as the H-terminated Si(111) surface in dry nitrogen (■). The SHG signal was recorded at the 0° azimuth of Figure 1.

surface. The measured reflectivity of  $20 \pm 2\%$  is in good agreement with the calculated reflectivity of 21% for Si, at 45° angle of incidence, for p-polarized light. The beam radius measured is the radius at which the intensity drops to  $1/e^2$  of its maximum value by definition. Therefore, the spot size is actually illuminated by the 86% of the beam's photons, 79% of which are adsorbed. For  $26 \mu\text{J}$  pulses ( $2 \text{ mJ/cm}^2$ ), corresponding to a photon flux of  $n = 8 \times 10^{18} \text{ photon s}^{-1} \text{ cm}^{-2}$ , the 0.7 ML oxygen coverage is achieved in 85 min. Using  $\sigma = \theta(t)/nt$  where  $\sigma$  is the photoreactive cross-section,  $\theta(t)$  is the oxygen coverage at time  $t$  (0.7 ML) and  $n$  is the photon flux in  $\text{photon s}^{-1} \text{ cm}^{-2}$ , the cross-section was determined to be  $(1.7 \pm 0.5) \times 10^{-23} \text{ cm}^2$ . The cross-section is several orders of magnitude smaller than the cross-section reported for direct photoexcitation of the Si-H bond [ $\sigma_{\text{H}} = (2.8 \pm 0.5) \times 10^{-21} \text{ cm}^2$ ].<sup>13</sup> The full monolayer of oxygen on Si(111) corresponds to  $8 \times 10^{14} \text{ O atom/cm}^2$ .<sup>35</sup> Thus, the number of oxygen atoms inserted into the Si-Si back-bonds per photon is  $\sim 10^{-8}$ . Equivalently, only one in every  $10^8$  incident photons causes a photoreaction.

Zhu et al. showed that 157 nm irradiation leads to dissociation of the Si-H bond by direct optical excitation.<sup>13</sup> However, the photon energy in the present study is not sufficient to excite the Si-H bond. Rather, a substrate-mediated mechanism should be considered for the observed oxidation process. The effect of oxygen and water vapor on the surface transformation process is highlighted by the lack of any apparent change in signal after 1 h of illumination in a dry nitrogen-purged environment (RH < 1%) (Figure 3). Careful analysis in fact shows that some oxidation does occur (<10<sup>-6</sup> ML/s) for an irradiance of  $6 \times 10^{19} \text{ photons s}^{-1} \text{ cm}^{-2}$  in a nitrogen environment. This suggests that experiments on H-terminated Si(111) surfaces requiring less than 5% oxidation can be carried out in 1 h under our irradiation conditions in dry nitrogen.

The effect of substrate heating on the SHG response was shown to be negligible as illustrated by the SHG recorded in ambient from oxide-covered Si(111) surfaces over a period of 1 h (Figure 3, ○). A slight decrease (<3%) in signal was observed and attributed to laser drift. The calculated temperature rise is 5 K for single pulse heating.<sup>36</sup> It was shown that for high repetition rate lasers, heat can be accumulated at the surface due to insufficient heat diffusion.<sup>36</sup> However, we estimated that for our 1 kHz laser repetition rate, this is not the case. The small temperature change (5 K) indicates that laser-induced thermal desorption of H is not responsible for the SH signal change. Temperatures in excess of 700 K are required for significant desorption from Si(111)-H.<sup>37,38</sup>

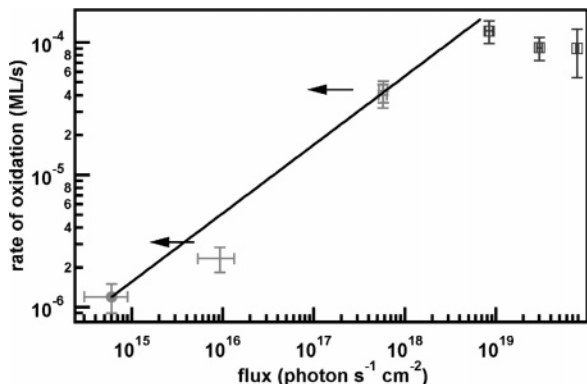


**Figure 4.** Dependence of the initial oxidation rate on photon flux. The rate of ambient oxidation (filled circle) was estimated from the photon flux of room light and the initial rate of oxidation in previous studies.<sup>31,32,35</sup> The rate of oxidation when a single spot on the sample was continuously irradiated by a flux of  $8 \times 10^{19}$ ,  $3 \times 10^{19}$ , and  $8 \times 10^{18}$  photons/cm $^2$  s is marked by open squares. The arrows indicate that the corresponding values are upper limits. The four data points with the lowest fluxes were fit (solid line) using equation  $y = b \times x^a$ , where the exponent  $a = 0.5 \pm 0.2$ .

To gain further insight into the possible mechanism of photooxidation, the dependence of the initial oxidation rate on the laser flux was investigated (Figure 4). The initial rate of oxidation appears to saturate at  $\sim 10^{-4}$  ML/s in the range explored. Photon fluxes greater than  $10^{19}$  photon cm $^{-2}$  s $^{-1}$  do not appear to accelerate the oxidation further. This might be because at high flux the supply of photons is no longer rate limiting. Rather, the abundance of other reactants, such as O<sub>2</sub> or H<sub>2</sub>O, limits the reaction rate. We found that as the flux is lowered below  $10^{18}$  photons cm $^{-2}$  s $^{-1}$ , the rate of oxidation does depend on the photon flux (Figure 4). However, the oxidation rate at low photon flux is representative of oxidation when random spots were irradiated and probed by SHG-RA (photon fluxes of  $\sim 10^{16}$  and  $7 \times 10^{17}$  photons s $^{-1}$  cm $^{-2}$ ). As it is unlikely that the exact same spot was irradiated and probed in the experiments that sampled the surface every few days, the flux shown here overestimates the number of photons received at any given spot. Therefore, the photoinduced oxidation for the points at the lowest flux is not readily comparable to the oxidation rate observed at high flux where a single spot was irradiated and probed (Figure 4, open squares). It should be noted that the samples were kept in a room with the lights on most of the time. The flux ambient photon was estimated to be  $6 \times 10^{14}$  photons cm $^{-2}$  s $^{-1}$ , which is about 4% of the irradiation that the samples received from the laser. (We assumed a 100 W visible light source and calculated the flux 2 m away from the source. One joule corresponds to  $\sim 3 \times 10^{18}$  photons at 500 nm. The surface area of a 2 m radius sphere is  $4\pi r^2 = 5 \times 10^5$  cm $^2$ . Thus, the flux is  $6 \times 10^{14}$  photon cm $^{-2}$  s $^{-1}$ .)

Ye et al. reported a nonlinear dependence of the rate constant of H abstraction with respect to input intensity at 532 and 1064 nm.<sup>19</sup> They suggested that abstraction of hydrogen is responsible for the observed SFG loss at 2083 cm $^{-1}$ .<sup>19</sup> The hydrogen abstraction was modeled with a first-order reaction, and the rate constant was determined with varying input power level at 532 and 1064 nm.<sup>19</sup> However, previous investigations suggest that the first step of the oxidation of the H-Si(100) surface is the insertion of oxygen into the Si-Si back-bonds.<sup>31,32</sup> This step does not remove hydrogen but would probably result in a significant perturbation of the SiH vibration monitored in the SFG experiment. In fact, FTIR studies of NH<sub>4</sub>F treated Si(111) showed that as the Si-H peak at 2083 cm $^{-1}$  disappears during

exposure to air, a broad feature at 2260 cm $^{-1}$  assigned to the O<sub>3</sub>Si-H species (Si bonded to three oxygens in its back-bonds) appears simultaneously.<sup>39</sup> Ye et al. scanned the infrared light from 2060 to 2110 cm $^{-1}$ , excluding the spectral region where the oxygen bonded Si-H stretches appear.<sup>19</sup> This might explain their interpretation of SiH loss as hydrogen abstraction. They suggested that a photoelectrochemical reaction is responsible for the desorption of the Si-H surface through photogenerated e-h pairs, concluding that water must also play a role.

There are significant differences between the results reported here and those of Ye et al. For example, Ye et al. observed a 60 min induction period, during which the intensity of the SFG peak did not change (relative humidity 40% and temperature 22 °C).<sup>19</sup> In contrast, the intensity of the Si-H stretch decreased to 70% of its initial value in the first hour during the oxidation of Si(111)-H as shown by FTIR (relative humidity 40%).<sup>39</sup> We did not observe an induction period. The phase  $\Delta_{AB}$ , the isotropic,  $A_{pp}$ , and the anisotropic,  $B_{pp}$ , parameters start to decrease slowly immediately after H termination, which indicates that the oxidation starts immediately upon illumination.<sup>24</sup>

In a recent paper, Cai et al. suggested a hole-mediated mechanism to be responsible for the photoreaction of Si-I surface with terminal alkenes.<sup>40</sup> Their mechanism is similar to that suggested by Ekwelundu et al. to be responsible for the desorption of CO, CO<sub>2</sub>, SO, and NO from Si(100).<sup>41</sup> The proposed mechanism involves the absorption of the 514 nm photons and the creation of e-h pairs in the Si bulk.<sup>40</sup> The electric field present at the interface separates the charges.<sup>40</sup> The n-type Si-I surface exhibits upward band bending; therefore, the photoexcited holes drift to the surface.<sup>40</sup> The surface Si atoms become positively charged and therefore susceptible to nucleophilic attack by reactive solution phase molecules.<sup>40</sup> In contrast, the p-type samples exhibit downward band bending; therefore, the photoexcited holes drift away from the surface.<sup>40</sup> The proposed mechanism was consistent with the greater reactivity of n-type opposed to p-type Si.<sup>40</sup>

Harper et al. observed reversible quenching of the visible photoluminescence of n-type porous Si and simultaneous slow photooxidation of the surface, when the sample was exposed to gaseous molecular oxygen.<sup>42</sup> Quenching was attributed to electron transfer from the luminescent chromophore in porous Si to an O<sub>2</sub> molecule physisorbed or weakly chemisorbed to a surface defect.<sup>42</sup> The proposed mechanism of photochemical oxidation involved the same photogenerated O<sub>2</sub><sup>-</sup> species produced during quenching.<sup>42</sup> Thus, the reversible quenching and photooxidation were linked together. Furthermore, the mechanisms of photooxidation proposed by Harper et al. and in this paper are similar, but the source of electrons must be different since no luminescent chromophore is present at the flat Si(111) surface. Thus, the electric field present at the Si(111)-H interface must be the driving force for the drift of electrons toward the interface.

Stewart et al. reported light-promoted (white light,  $\lambda > 400$  nm, 20 mW/cm $^2$ ) hydrosilylation reaction using photoluminescent nanocrystalline silicon.<sup>43</sup> They found that the reaction is unique to photoluminescent silicon and does not function on nonemissive material, i.e., flat silicon.<sup>43</sup> Thus, a reaction mechanism involving a reactive center generated from a surface-localized exciton was proposed.<sup>43</sup> However, our data suggest that reactivity of the silicon surface induced by  $\lambda > 400$  nm photons is not unique to porous silicon. Stewart et al. did not observe a photoassisted reaction on flat Si surfaces because the photon flux was 3 orders of magnitude smaller than in our studies (20 mW/cm $^2$  vs 2 W/cm $^2$ ). Photons (800 nm) can

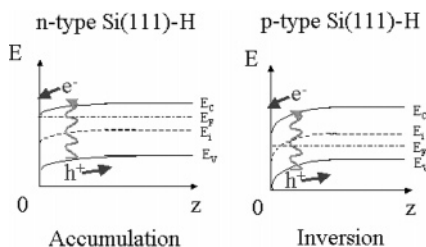


**Figure 5.** Schematic illustration of energy bands and movement of free carriers (electrons,  $e^-$ ; and holes,  $h^+$ ) upon excitation with 800 nm photons at n-type and p-type Si(111)-H. The n-type Si(111)-H is in the accumulation regime, and the p-type Si(111)-H is in the inversion regime.<sup>35,44–46</sup>  $E_c$  is the conduction band edge,  $E_v$  is the valence band edge,  $E_i$  is the midgap,  $E_F$  is the Fermi level, and  $z$  is the distance perpendicular to the surface.

accelerate oxidation of flat Si(111)-H surface when the photons are supplied in a high enough density.

The photon energy (1.55 eV) used in this study is enough to create electron–hole pairs through the indirect transition of Si (1.1 eV). Assuming a mechanism similar to that proposed by Cai et al., the electron must be the reactive species in the oxidation reaction of Si(111)-H, not the holes as in the proposed mechanism for the reaction of Si(111)-I surface with olefins.<sup>40</sup> This is the consequence of the band bending. For n-type Si(111)-H, an accumulation layer was measured.<sup>44–46</sup> Thus, the drift of electrons is expected toward the surface (Figure 5). For p-type Si(111)-H, an inversion layer was measured.<sup>35,46</sup> Thus, electrons are expected to drift toward the surface as well (Figure 5). Therefore, an enhancement of the oxidation rate is expected for illuminated p-type Si(111)-H, if the above proposed mechanism is correct.

Let us consider what happens under our experimental conditions. The 1.8 mJ/cm<sup>2</sup> pulse creates as many as  $6 \times 10^{18}$  cm<sup>-3</sup> e–h pairs. The penetration depth of 800 nm light at Si surface (45° angle of incidence, p-polarized light) is 10  $\mu\text{m}$ . The length of the space charge layer is estimated to be 830 nm for the n-type, lightly P-doped samples ( $30 \Omega \text{ cm}$ ,  $N_D \sim 4 \times 10^{14} \text{ cm}^{-3}$ ) used in this study. Therefore, approximately 10% of the free carriers fall within the space charge layer and can diffuse toward the surface. Thus, approximately  $10^{18}$  cm<sup>-2</sup> electrons are available at the surface to react with the reactive species of the ambient, i.e., O<sub>2</sub> or H<sub>2</sub>O. Wade et al. have suggested that the presence of the excess electrons at the Si(111)-H surface can help the one-electron transfer reaction to O<sub>2</sub> (O<sub>2</sub> + e<sup>-</sup> → O<sub>2</sub><sup>·-</sup>) take place in 40% NH<sub>4</sub>F solution containing oxygen.<sup>46</sup> Even though this mechanism was proposed to explain the etch-pit formation in 40% NH<sub>4</sub>F solution containing oxygen, the authors have pointed out that this mechanism may lead to oxide formation in the absence of fluoride in air-containing water or in humid air.<sup>46</sup> Therefore, a mechanism involving photogenerated e–h pairs is a plausible explanation of the observed photoenhanced oxidation. The above-proposed role of photons in the oxidation of Si(111)-H suggests a linear dependence of the initial oxidation rate on the input intensity. Furthermore, an enhancement of initial oxidation rate for p-type Si(111)-H by 800 nm photons would be expected. Further studies on the dependence of photooxidation on doping are in progress.

## Conclusion

We have investigated the photooxidation of Si(111)-H surface using SHG at 800 nm. We found that 800 nm photons accelerate the initial stage of oxidation of Si(111)-H in ambient. The cross-section of the photoinduced process was found to be

( $1.7 \pm 0.5$ ) × 10<sup>-23</sup> cm<sup>2</sup>. The power dependence of the initial oxidation rate showed that the process is saturated for photon fluxes > 10<sup>19</sup> photon cm<sup>-2</sup> s<sup>-1</sup>. The exclusion of water and oxygen slows down the oxidation process, indicating that both play a role as reactants in this process. The direct photoexcitation of Si–H bond or H desorption due to substrate heating was excluded as a possible mechanism. No induction period was observed in contrast to Ye et al., which we attributed to the higher flux used in this study.

**Acknowledgment.** We acknowledge the generous support of the DOE, Office of Basic Energy Sciences.

## References and Notes

- Doren, D. J. Kinetics and dynamics of hydrogen adsorption and desorption on silicon surfaces. *Adv. Chem. Phys.* **1996**, 95 (Surface Properties), 1–60.
- Waltenburg, H. N.; Yates, J. T. Surface chemistry of silicon. *Chem. Rev.* **1994**, 95 (5), 1589–1673.
- Higashi, G. S.; Chabal, Y. J.; Trucks, G. W.; Raghavachari, K. Ideal hydrogen termination of the Si(111) surface. *Appl. Phys. Lett.* **1990**, 56 (7), 656–658.
- Wolkow, R. A. Controlled molecular adsorption on silicon: Laying a foundation for molecular devices. *Annu. Rev. Phys. Chem.* **1999**, 50, 413–441.
- Yates, J. T. A new opportunity in silicon-based microelectronics. *Science* **1998**, 279 (5349), 335–337.
- Hamers, R. J.; Hovis, J. S.; Lee, S.; Liu, H.; Shan, J. Formation of ordered, anisotropic organic monolayers on the Si(001) surface. *J. Phys. Chem. B* **1997**, 101 (9), 1489–1492.
- Teplyakov, A. V. M.; Kong, J.; Bent, S. F. Diels–Alder reactions of butadiens with the Si(100)-2 × 1 surface as a dienophile: Vibrational spectroscopy, thermal desorption and near edge X-ray absorption fine structure studies. *J. Chem. Phys.* **1998**, 108 (11), 4599–4606.
- Buriak, J. M. Organometallic chemistry on silicon surfaces: Formation of functional monolayers bound through Si–C bonds. *Chem. Commun.* **1999**, (12), 1051–1060.
- Linford, M. R.; Chidsey, C. E. D. Alkyl monolayers covalently bonded to silicon surfaces. *J. Am. Chem. Soc.* **1993**, 115 (26), 12631–12632.
- Shen, T. C.; Wang, C.; Abeln, G. C.; Tucker, J. R.; Lyding, J. W.; Avouris, P.; Walkup, R. E. Atomic-scale desorption through electronic and vibrational-excitation mechanisms. *Science* **1995**, 268 (5217), 1590–1592.
- Pusel, A.; Wetterauer, U.; Hess, P. Photochemical hydrogen desorption from H-terminated silicon(111) by VUV photons. *Phys. Rev. Lett.* **1998**, 81 (3), 645–648.
- Vondrak, T.; Zhu, X. Y. Direct photodesorption of atomic hydrogen from Si(100) at 157 nm: Experiment and simulation. *J. Phys. Chem. B* **1999**, 103 (23), 4892–4899.
- Vondrak, T.; Zhu, X. Y. Dissociation of a surface bond by direct optical excitation: H–Si(100). *Phys. Rev. Lett.* **1999**, 82 (9), 1967–1970.
- Radeke, M. R.; Carter, E. A. Ab initio dynamics of surface chemistry. *Annu. Rev. Phys. Chem.* **1997**, 48, 243–270.
- Steckel, J. A.; Phung, T.; Jordan, K. D.; Nachtigall, P. Concerted use of slab and cluster models in an ab initio study of hydrogen desorption from the Si(100) surface. *J. Phys. Chem. B* **2001**, 105 (18), 4031–4038.
- Bobrov, K.; Comtet, G.; Dujardin, G.; Hellner, L. Electronic structure of partially hydrogenated Si(100)-(2 × 1) surfaces prepared by thermal and nonthermal desorption. *Phys. Rev. Lett.* **2001**, 86 (12), 2633–2636.
- Cicero, R. L.; Linford, M. R.; Chidsey, C. E. D. Photoreactivity of unsaturated compounds with hydrogen-terminated silicon(111). *Langmuir* **2000**, 16 (13), 5688–5695.
- Laarhoven, L. J. J.; Mulder, P.; Wayner, D. D. M. Determination of bond dissociation enthalpies in solution by photoacoustic calorimetry. *Acc. Chem. Res.* **1999**, 32 (4), 342–349.
- Ye, S.; Saito, T.; Nihonyanagi, S.; Uosaki, K.; Miranda, P. B.; Kim, D.; Shen, Y. R. Stability of the Si–H bond on the hydrogen-terminated Si(111) surface studied by sum frequency generation. *Surf. Sci.* **2000**, 476 (1–2), 121–128.
- Guyot-Sionnest, P.; Dumas, P.; Chabal, Y. J. Lifetime of an adsorbate–substrate vibration measured by sum frequency generation: Hydrogen on silicon(111). *J. Electron Spectrosc. Relat. Phenom.* **1990**, 54–55, 27–38.
- Palik, E. D., Ed. *Handbook of Optical Constants of Solids*; Academic: San Diego, 1998.
- Luo, H.; Chidsey, C. E. D.; Chabal, Y. Infrared spectroscopy of covalently bonded species on silicon surfaces: Deuterium, chlorine, and cobalt tetracarbonyl. *Mater. Res. Soc. Symp. Proc. Vol.* **1997**, 477, 415.

- (23) Dumas, P.; Chabal, Y. J. Electron-energy-loss characterization of the H terminated Si(111) and Si(100) surfaces obtained by etching in NH<sub>4</sub>F. *Chem. Phys. Lett.* **1991**, *181* (6), 537.
- (24) Bodlaki, D.; Borguet, E. In situ second harmonic generation measurements of the stability of Si(111)–H and kinetics of oxide regrowth in ambient. *J. Appl. Phys.* **2004** *95* (9), 4675–4680.
- (25) Lupke, G.; Bottomley, D. J.; Vandriel, H. M. 2nd-Harmonic and 3rd-harmonic generation from cubic centrosymmetric crystals with vicinal faces—Phenomenological theory and experiment. *J. Opt. Soc. Am. B—Opt. Phys.* **1994**, *11* (1), 33–44.
- (26) Bodlaki, D.; Borguet, E. Picosecond infrared optical parametric amplifier for nonlinear interface spectroscopy. *Rev. Sci. Instrum.* **2000**, *71* (11), 4050–4056.
- (27) van Driel, H. M. Kinetics of high-density plasmas generated in Si by 1.06 and 0.53-μm picosecond laser pulses. *Phys. Rev. B* **1987**, *35* (15), 8166–8176.
- (28) Fomenko, V.; Lami, J. F.; Borguet, E. Non-quadratic second harmonic generation from semiconductor-oxide interfaces. *Phys. Rev. B* **2001**, *63*, 121316.
- (29) Litwin, J. A.; Sipe, J. E.; Van Driel, H. M. Picosecond and nanosecond laser-induced second-harmonic generation from centrosymmetric semiconductors. *Phys. Rev. B: Condens. Matter* **1985**, *31* (8), 5543–5546.
- (30) Gräf, D.; Grundner, M.; Schulz, R. Reaction of water with hydrofluoric acid treated silicon(111) and (100) surfaces. *J. Vac. Sci. Technol., A* **1989**, *7* (3, Part 1), 808–13.
- (31) Gräf, D.; Grundner, M.; Schulz, R.; Mühlhoff, L. Oxidation of HF treated Si wafer surfaces in air. *J. Appl. Phys.* **1990**, *68* (10), 5155–5161.
- (32) Houston, M. R.; Maboudian, R. Stability of ammonium fluoride-treated Si(100). *J. Appl. Phys.* **1995**, *78* (6), 3801.
- (33) Kluth, G. J.; Maboudian, R. Oxidation mechanism of the ammonium-fluoride-treated Si(100) surface. *J. Appl. Phys.* **1996**, *80* (9), 5408–5414.
- (34) Morita, M.; Ohmi, T.; Hasegwa, E.; Kawakami, M.; Suma, K. Control factor of native oxide growth on silicon in air or in ultrapure water. *Appl. Phys. Lett.* **1989**, *56* (7), 562–564.
- (35) Angermann, H.; Herion, W.; Roseler, A. Wet-chemical conditioning of silicon: Electronic properties correlated with the surface morphology.
- In *Silicon-Based Materials and Devices*; Nalwa, H. S., Ed.; Academic Press: New York, 2001; pp 267–298.
- (36) Dadap, J. I.; Hu, X. F.; Russell, N. M.; Ekerdt, J. G.; Lowell, J. K.; Downer, M. C. Analysis of second-harmonic generation by unamplified, high-repetition-rate, ultrashort laser pulses at Si(001) interfaces. *IEEE J. Sel. Top. Quantum Electron.* **1995**, *1* (4), 1145–1155.
- (37) Sinniah, K.; Sherman, M. G.; Lewis, L. B.; Weinberg, W. H.; Yates, J. T., Jr.; Janda, K. C. New mechanism for hydrogen desorption from covalent surfaces: The monohydride phase on silicon(100). *Phys. Rev. Lett.* **1989**, *62* (5), 567–70.
- (38) Pietsch, G. J. Hydrogen on Si—Ubiquitous surface termination after wet-chemical processing. *Appl. Phys. A: Mater. Sci. Process.* **1995**, *60* (4), 347–363.
- (39) Niwano, M.; Kageyama, J.; Kurita, K.; Kinashi, K.; Takahashi, I.; Miyamoto, N. Infrared-spectroscopy study of initial-stages of oxidation of hydrogen-terminated Si surfaces stored in air. *J. Appl. Phys.* **1994**, *76* (4), 2157–2163.
- (40) Cai, W.; Lin, Z.; Strother, T.; Smith, L. M.; Hamers, R. J. Chemical modification and patterning of iodine-terminated silicon surfaces using visible light. *J. Phys. Chem. B* **2002**, *106* (10), 2656–2664.
- (41) Ekwelundu, E.; Ignatiev, A. Low energy photodesorption from Si(100) exposed to CO, CO<sub>2</sub>, O<sub>2</sub>, NO and SO<sub>2</sub>. *Surf. Sci.* **1987**, *179*, 119–131.
- (42) Harper, J.; Sailor, M. J. Photoluminescence quenching and the photochemical oxidation of porous silicon by molecular oxygen. *Langmuir* **1997**, *13*, 4652–4658.
- (43) Stewart, M. P.; Buriak, J. M. Exciton-mediated hydrosilylation on photoluminescent nanocrystalline silicon. *J. Am. Chem. Soc.* **2001**, *123*, 7821–7830.
- (44) Allongue, P.; Kieling, V.; Gerischer, H. Etching mechanism and atomic structure of H–Si(111) surfaces prepared in NH<sub>4</sub>F. *Electrochim. Acta* **1995**, *40*, 1353.
- (45) Angermann, H.; Kliefoth, K.; Flietner, H. Preparation of H-terminated Si surfaces and their characterization by measuring the surface state density. *Appl. Surf. Sci.* **1996**, *104/105*, 107–112.
- (46) Wade, C. P.; Chidsey, C. E. D. Etch-pit initiation by dissolved oxygen on terraces of H–Si(111). *Appl. Phys. Lett.* **1997**, *71* (12), 1679.